International Journal of Advance Research and Innovation
Vol. 2(2), Apr-Jun 2014, pp. 185-192
Doi 10.51976/ijari.221425

**Article Info**
Received 02 Jan 2014 | Revised Submission 10 Jan 2014 | Accepted 28 May 2014 | Available Online 15 Jun 2014

# Simulation of Single Slope Solar Still at Different Inclinations using CFD

*Amrik Singh* and M. K Mittal***

**ABSTRACT**

*The solar still is the one of the good and cost effective method for obtaining the fresh water from contaminated water. Hence for increasing the performance of solar still it is necessary to model and investigate the effect of different parameters as condensing cover. In this paper two condensing covers at inclination 150 and 300 slope studied to analyze the effect on rate of evaporation. Simulation is carried out from 40-600C with 20C interval. For 150 and 300 inclination various contours have been plotted and studied for each simulation. There is a good agreement between simulated data and available experimental data. Hence CFD is powerful tool in design of solar still and studying effective parameters on the performance.*

***Keywords*** *CFD; Solar Still; Inclination.*

## 1.0 Introduction

Distillation is a process which is used to obtain fresh water from salty, brackish or contaminated water. Without fresh water human life is not possible even industries and agriculture also need fresh water. Earlier fresh water is easily available from rivers, lakes and ponds in plenty. Now it's becoming scarce because of industrialization. Growing population leads to assumption that by the year 2025 two thirds of the population will lack sufficient fresh water [1]. The areas with the water shortages are the warm, arid countries in the northern Africa and southern Asia within the latitudes 15-35ºN [2]. Sunlight is one of several forms of heat energy that can be used to power the process of water purification [3].

It is difficult to use solar thermal energy in large scale plants because of low thermal efficiency and considerable land area required. This technology is suitable for small scale where supply of conventional energy is scarce [6-7]. This technology is use full because of low environment impact as well as easy operation and maintenance [8-9].

Jadav compared black granite basin with iron steel basin and concluded that productivity of black granite basin is 38% more than iron steel basin. Omar find the best factor enhancing the productivity of solar still by studying various operational parameters like solar intensity, absorptivity and transmitivity etc. In this paper two phase model was developed using ANSYS CFX for condensation and evaporation and simulation results are compared with the available experimental data.

## 2.0 Heat Transfer Coefficient Analysis

In solar distillation system, the heat transfer can be classified in terms of external and internal modes [10]. In this case convective heat transfer occurs simultaneously with evaporative heat transfer and these two heat transfer processes are independent of radiative heat transfer.

The gas phase above the liquid water is convected to the condensing cover by the action of buoyancy force caused by density variation due to temperature difference between water surface and condensing cover temperature.

Rate of heat transfer from the water surface to the glass cover by convection in the upward direction through humid fluid can be estimated by

$$\dot{q}_{cw}=h_{cw}(T_w - T_g) \qquad (1)$$

$h_{cw}$ is the convective heat transfer coefficient.

Dunkle's [5] relation for convective heat transfer coefficient from water to glass, hCW is used.

**Corresponding Author: Department of Mechanical Engineering, Thapar University Patiala Punjab, India (E-mail amriksingh200@gmail.com)*
***Department of Mechanical Engineering, Thapar University Patiala Punjab, India*

$$h_{cw} = 0.884\left[T_w - T_g + \frac{(P_w - P_g)(T_w + 273)}{268.9\times10^3 - P_w}\right]^{1/3}$$

(2)The evaporative heat transfer coefficient, hew from water to glass is given by Eq. 3

$$h_{ew} = 0.01623 \times h_{cw} \times \left(\frac{P_w - P_g}{T_w - T_g}\right) \quad (3)$$

For mass transfer model, interfacial mass flux is used [15]. It was assumed that the rate of water evaporation is equal to the rate of fresh water production. Therefore mass flux equation between the two phases is

$$\dot{m}_{ew} = \frac{q_{ew}\times A_w \times t}{L} \quad (4)$$

Where

$$\dot{q}_{ew} = h_{ew}(T_w - T_g) \quad (5)$$

The accurate estimation of internal heat transfer coefficients is a critical step for the prediction of a solar still performance. The convective heat transfer coefficient is given by the Nusselt number, which is the ratio of convective to conductive heat transfer across a boundary.

$$Nu = \frac{h_{cw}}{k_v} * L_v = C(Gr.Pr)^n \quad (6)$$

Hence

$$h_{cw} = \frac{K_v}{L_v} * C(Gr.Pr)^n \quad (7)$$

$$Gr = \frac{\beta g L_v^3 \rho^2 \Delta T}{\mu^2} \quad (8)$$

$$Pr = \frac{\mu \cdot C_p}{K_v} \quad (9)$$

$$T_v = (T_w + T_g)/2 \quad (10)$$

Table 1 shows the Temperature dependent physical properties of vapour. Calculation of constants C and n in equation (7) were based on regression analysis of the predicted results of CFD using Kumar and Tiwari [4] method. The convective heat transfer coefficient is evaluated from Eq.7 using the values of obtained C and n. The evaporative heat transfer coefficient in the system and condensed water rate are obtained from Eqs. (3) and (4) By substituting hcw from Eq. (7) into Eq (3) we have

$$h_{ew} = 0.01623 \times \frac{K_v}{L_v} \times C(GrPr)^n \times \left(\frac{P_w - P_g}{T_w - T_g}\right) \quad (11)$$

Further substituting $h_{ew}$ into Eq. (5) and then $\dot{q}_{ew}$ into Eq. (4) we get

$$\dot{m}_{ew} = \frac{0.01623}{L} \times \frac{K_v}{L_v} \times A_w \times t \times (P_w - P_g) \times C(GrPr)^n \quad (12)$$

Therefore

$$\dot{m}_{ew} = R \cdot C(GrPr)^n \quad (13)$$

$$\frac{\dot{m}_{ew}}{R} = C(GrPr)^n \quad (14)$$

Where

$$R = \frac{0.01623}{L} \times \frac{K_v}{L_v} \times A_w \times t \times \left(P_w - P_g\right) \quad (15)$$

$$y = mx + C_o \quad (16)$$

Taking the logarithms of both sides of Eq. (14)

$$y = ln\left(\frac{\dot{m}_{ew}}{R}\right) \; C_o = ln\, C, x = ln(GrPr) \; and \; m = n \quad (17)$$

using linear regression analysis the constants C and n evaluated.

$$m = \frac{N(\sum XY) - (\sum X)(\sum Y)}{N(\sum X^2) - (\sum X)^2} \quad (18)$$

$$C_o = \frac{(\sum Y)(\sum X^2) - (\sum X)(\sum XY)}{N(\sum X^2) - (\sum X)^2} \quad (19)$$

$$C = exp(C_o) \quad (20)$$

$$n = m \quad (21)$$

**Table 1: Temperature Dependent Physical Properties of Vapour [4]**

| Quantity | Symbol | Expression |
|---|---|---|
| Specific heat | $C_p$ | $C_p = 999.2 + 0.1434 \times T_i + 1.101 \times 10^{-4} \times T_i^2 - 6.7581 \times 10^{-3} \times T_i^3$ |
| Density | ρ | $353.44/(T_i + 273.15)$ |
| Thermal conductivity | $K_v$ | $0.0244 + 0.7673 \times 10^{-4} \times T_i$ |
| Viscosity | μ | $1.718 \times 10^{-5} + 4.620 \times 10^{-8} \times T_i$ |
| Latent heat of vaporization of water | $L$ | $3.1615 \times 10^6 \times [1 - (7.616 \times 10^{-4} \times T_i)]$; for $T_i > 70^0C$<br>$2.4935 \times 10^6 \times [1 - 9.4779 \times 10^{-4} T_i + 1.3132 \times 10^{-7} \times T_i^2 - 4.7974 \times 10^{-9} \times T_i^3]$; for $T_i < 70^0C$ |
| Partial saturated vapour pressure at condensing cover temperature | $P_g$ | $Exp[25.317 - 5144/(T_g + 273)]$ |
| Partial saturated vapour pressure at water temperature | $P_w$ | $Exp[25.317 - 5144/(T_w + 273)]$ |
| Expansion factor | β | $1/(T_i + 273.15)$ |

### 3.0 Flow Geometry

The schematic diagram of experimental set up of Anil Kr. Tiwari, G. N. Tiwari is shown in Fig 1 Evaporative surface area of the condensing cover is 250mm*365mm. For simulation purpose two condensing covers are taken at inclination 150 and 300 dimensions are shown in the table 2. Geometric modal of solar still is created using ANSYS CAD module and this geometric modal is imported to the ANSYS meshing module to generate the meshing. Geometry is shown in figures 3.2 and 3.3 for 150 and 300 inclinations respectively.

**Table 2: Specification of Two Condensing Covers**

| Sr. no | Dimensions | Inclination, mm | |
|---|---|---|---|
| | | 15° | 30° |
| 01 | Length | 365 | 365 |
| 02 | Lower height | 70 | 70 |
| 03 | Higher height | 185 | 295 |
| 04 | Width | 250 | 250 |

### 4.0 Boundary Conditions

Mesh files of solar still are then imported to the CFX Pre. In CFX pre physics and boundary conditions are applied on the domain is explained to solve the continuity and momentum equation. A two phase domain is created in the (VOF) framework for liquid water and mixture of water vapour and air. Evaporation process is modeled as laminar at quasi steady, accounting for thermal energy heat transfer while considering the effects of buoyancy. A distinct interface between vapor and liquid phases exists, hence both phases are continuous. To transfer heat, two resistance model is taken zero resistance model is taken for gas phase and heat transfer coefficient for water phase. It was assumed that bottom temperature is equal to water bath temperature. Distillate collector temperature is equal to glass temperature. For drop formation on the condensing cover adhesion forces are taken. All sides are assumed adiabatic so there is no heat loss to surrounding. No slip boundary condition is specified for liquid phase and free slip boundary condition is specified for Vapour phase

**Fig 1: A Schematic Diagram of Experimental Setup of Solar Still [4]**

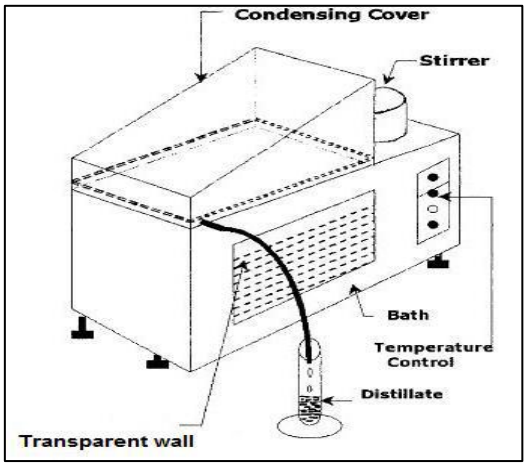


**Table 2. Boundary Condition and Initial Condition**

| Location | Boundary Type | Boundary Details | Comments |
|---|---|---|---|
| Top (condensing cover) | Wall | Fixed temperature wall | Condensing wall for drop formation adhesion forces were taken into account |
| Bottom | Wall | Temperature = $40^0$ C to $60^0$ C with $2^0$C interval | Bottom temperature is equal to the bath temperature from which heat is given to the water |
| All four Sides<br>Long wall<br>Small wall<br>Front<br>Back | Wall | Adiabatic | No slip boundary condition specified for liquid phase and free slip for gas phase and all walls are also set to be adiabatic so that there is no heat loss to the surrounding |
| Distillate Collector | Wall | Distillate collector temperature = Glass cover temperature | To collect condensed water |

### 5.0 Meshing Detail

Geometry is imported to ansys meshing module and meshing is done. Unstructured mesh of type tetrahedral is used. A mesh independence test was conducted to ensure the results obtained are accurate and reliable. Test for grid independence is

done and jacobian for meshing is taken 0.8. Fig 2 and 3 show meshing details

**Fig 2: 3D Unstructured Mesh for 150 Inclination**

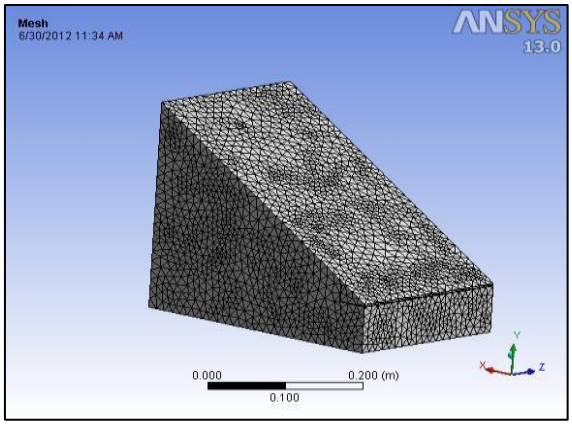


**Fig 3: 3D Unstructured Mesh for 300 Inclination**

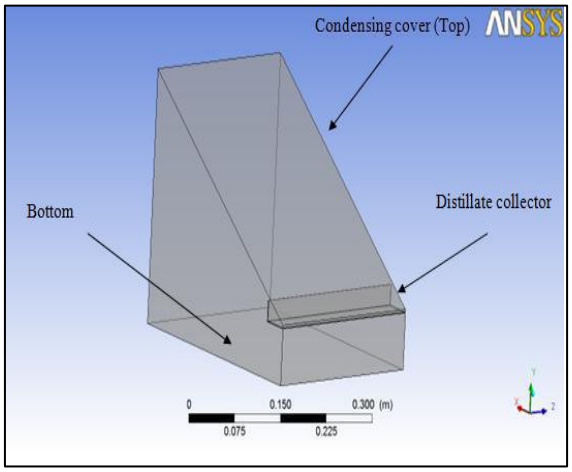


**Fig 4: Domain in CFX Pre**

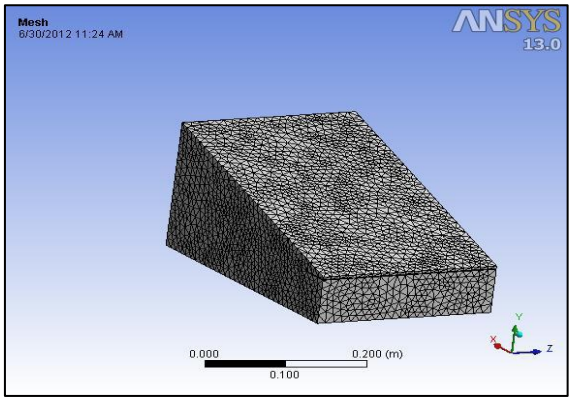


**Fig 5: Water Temperature Predicted by the CFD Simulation and Experimental Data for i) 150 Inclination ii) 300 Inclination**

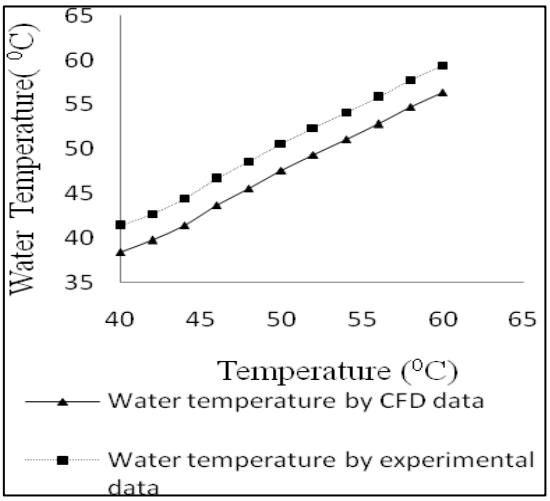


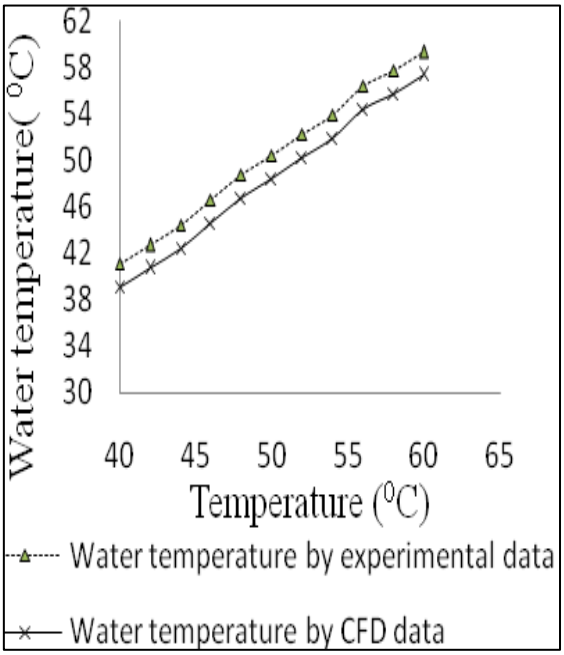


## 6.0 Experimental Validation

### 6.1 Water temperature

From the above results water temperature predicted by CFD simulation is compared with available experimental data of Kumar and Tiwari [4] for 150 and 300inclination shown in figure 5. This Fig has been drawn with Water temperature as ordinate and Bath temperature as abscissa. Water temperature is in good agreement with experimental

### 6.2 Production rate of water

data. The average error of water temperature is 8% and 6 % respectively from 400 to 600C with rise in bath temperature.

It was assumed that the amount of water evaporated is equal to the rate of water production Kg/m2 sec. In other words the amount of water evaporated is equal to the amount of water condensed. The same amount of water is collected in distillate channel. To represent the mass flow images of contour is shown in fig 6 for 150 inclination.

**Fig 6: Water Mass Flow Predicted by CFD Simulation.**

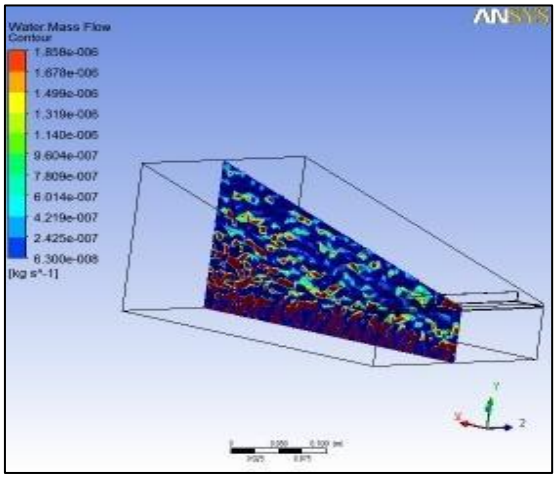


**Fig 7: The Rate of Fresh Water Production From Experimental Data and Simulation Result for 150 Inclination**

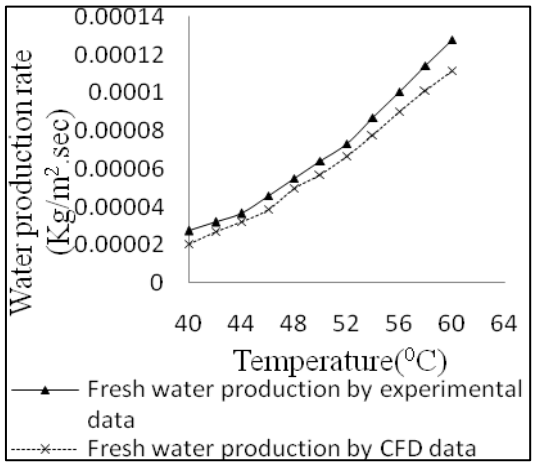


Water production rate by CFD data is also in good agreement with Experimental data. In the starting water production rate is low as the bath temperature is low. The average error for production rate is 11.8% for 150 slope and 7.6% for 300slope as shown in figure 8.

**Fig 8: The Rate of Fresh Water Production From Experimental Data and Simulation Result for 300 Inclination**

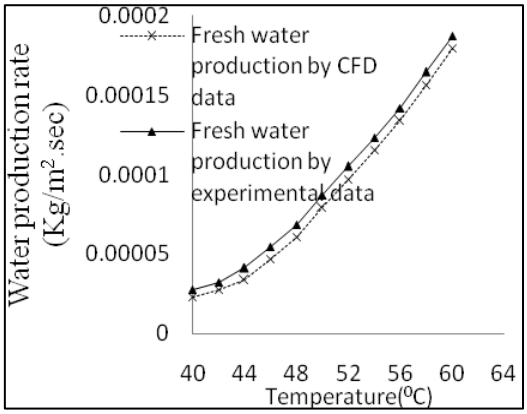


**Fig 9: Show the Condensed Water Droplets on the Glass as the Water Heated. Water Volume Fraction on the Glass for (I) 150 Inclination**

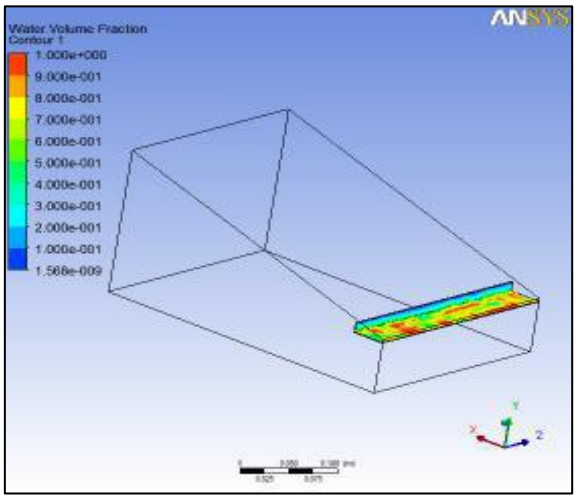


The water temperature is higher than glass cover temperature. Temperature difference between water vapour and glass leads to vapour condensation on the glass surface. For drop formation on condensing cover adhesion forces are taken into account. Droplets slip down and get collected in the trace as shown in figure 10.It is obvious that gas and liquid phase are completely apart and their interface is distinct. As shown in Figs 9 and 10 Liquid are seen only at the bottom, top and distillate collector.

**Fig 10: Water Volume Fraction Contour on Distillate Collector For (I) 150 Inclination**

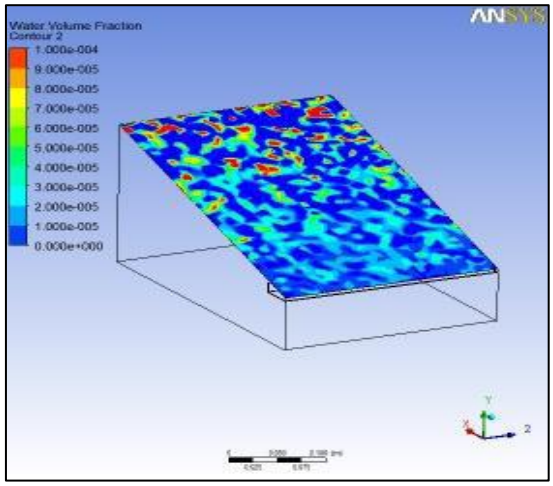


### 6.3 Heat transfer coefficient analysis

Heat transfer is due to the buoyancy force. The equations are already discussed in the starting. Gas phase moves on circular path lines between bottom and the glass. Warm water moves upward as their density decreases and the portion of vapour gets

**Fig 11: Gas Mixture Velocity on a Plane Inside the Solar Still for 300 Inclination**

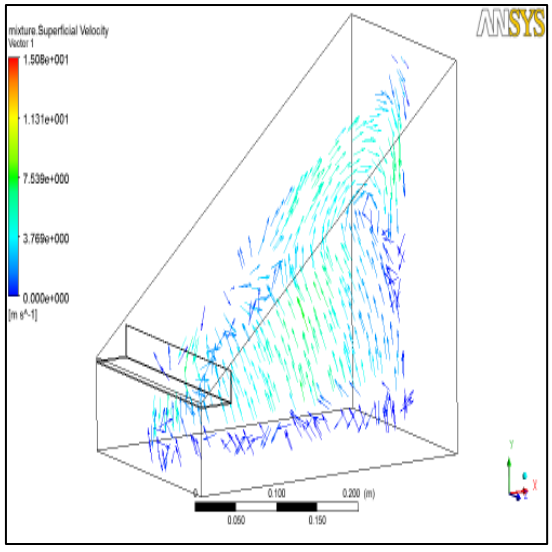


condensed on the top where it cools down and gets heavier. It forces the lighter warm vapour towards the glass and hence free convection heat transfer mechanism takes place as shown in Figs 11.

**Fig 12. Variation of (Hcw) for 150 Slope of the Condensing Cover**

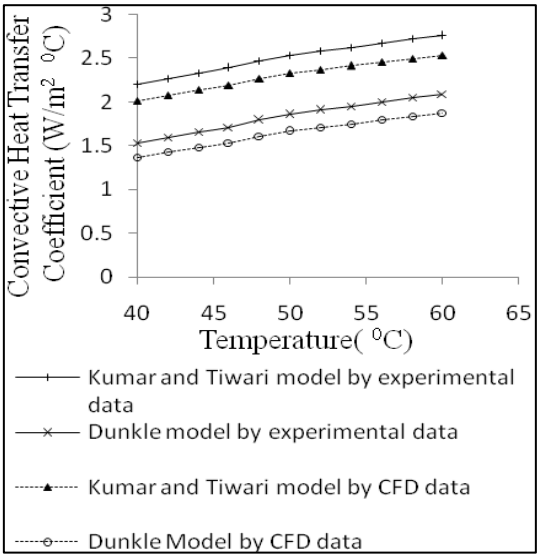


**Fig 13: Variation of Evaporative Heat Transfer Coefficient (Hew) Within Temperature Range of 400- 600C for 150 Slope of the Condensing Cover**

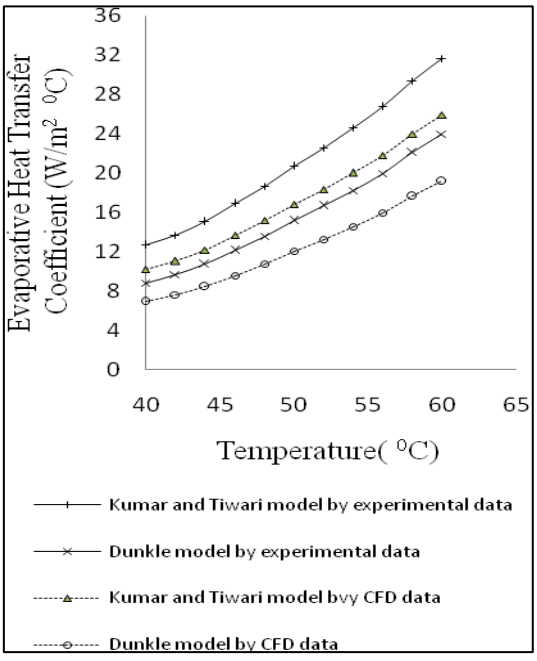


It was observed that experimental results of convective heat transfer coefficient and evaporative heat transfer coefficient for both inclinations nearly match with the heat transfer coefficient in simulation at all bath temperature from 400-600C. CFD data

obtained by both models under predict as shown in figure 13, 14 and 15. But the trend they are following is the same as that of experimental data with certain error.

**Fig 14: Variation of (Hcw) Within Temperature Range of 400- 600C for 300 Slope of the Condensing Cover**

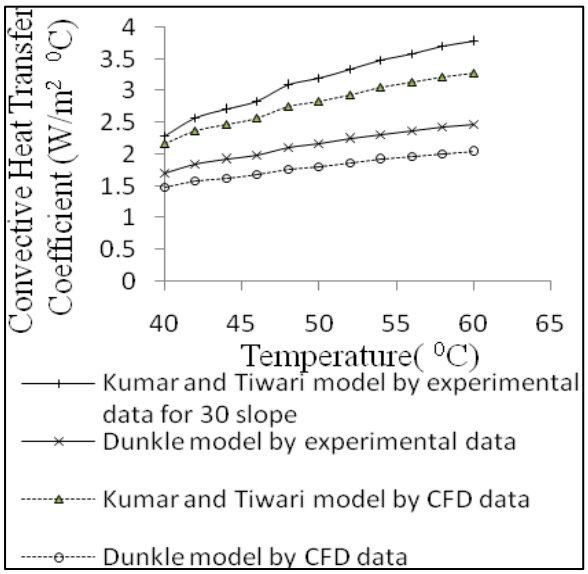


**Fig 15: Variation of Evaporative Heat Transfer Coefficient (Hew) Within Temperature Range of 400- 600C For 300 Slope of the Condensing Cover**

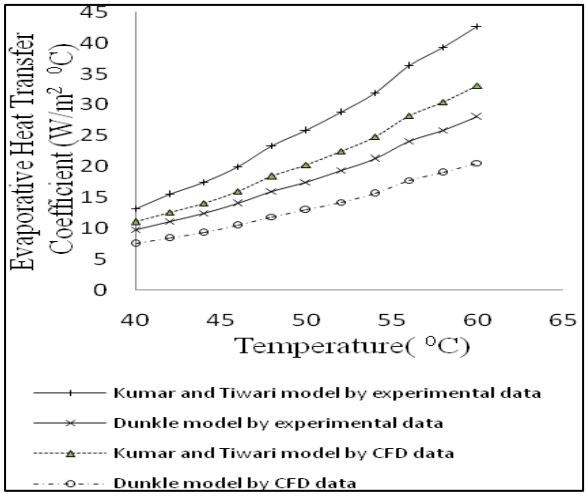


**7.0 Conclusion**

Simulation work is done on ANSYS CFX 13. Simulation of evaporation process is done on a single slope solar still. Different sets of simulation are done by varying the temperature of top and bottom according to experimental data. The behavior of phase change and temperature distribution is observed due to evaporation. The temperature of water obtained by CFX and mass yield is compared with the available experimental data. Two inclination of condensing cover at 150 and 300 are taken for simulation.

By plotting the curves of mass of water produced, convective and evaporative heat transfer coefficient it is determined that condensing cover at 300 inclination gives higher yield as compared to condensing cover at 150 inclination.) Curves for convective and evaporative heat transfer coefficient are plotted.

It is observed that condensing cover at inclination 300 obtain the high convective and evaporative heat transfer coefficient. The condensing cover at 300 inclination gives about 29.4% higher yield than 150 inclination. Hence CFD is powerful tool in design of solar still and studying effective parameters on the performance.

**Reference**

[1] UNEPb (United Nations Energy Programme)http //www.unep.org/geo2000/english/0046.htm [2003-06-09]

[2] Hussain A.K.M. Solar energy utilization in Libya for seawater desalination. Proceedings at the ISES Solar World Congress 2003, Gothenburg.

[3] Garzia-Rodriguez L, et al. Comparison of solar technologies for applications in seawater desalination. Desalination 2002 142, 135-142

[4] AK Tiwari, GN Tiwari, Effect of the condensing cover's slope on internal heat and mass transfer in distillation an indoor simulation. Desalination 180 (73-88), 2005

[5] RV Dunkle, Solar water distillation, the roof type still and a multiple effect diffusion still, International Developments in Heat Transfer, ASME, Proc. International Heat

Transfer, Part V, University of Colorado, 1961, 895

[6] Naim, M., et al. Non-conventional solar stills Part 1 Non-conventional solar stills with charcoal particles as absorber medium. Desalination 2002 153, 55-64

[7] Naim, M., et al. Non-conventional solar stills Part 2 Non-conventional solar stills

with energy storage medium. Desalination 2002 153, 71-80

[8] Garzia-Rodriguez L .Seawater desalination driven by renewable energies a review. Desalination 2002 143, 103-113

[9] Fath H.E.S. Solar distillation a promising alternative for water provision with free energy, simple technology and clean environment. Desalination 1998 116, 45-56

[10] FP Incropera, D Witt, DP Bergman, A. S Lavine, Fundamentals of heat and mass transfer.6th edition. New Jersey John Wiley and Sons, 2007

[11] CFX User Manual, ANSYS, Inc. Modeling, CFX 13.0 Solver.

[12] VJ Madhav, Performance of Black Granite Basin Solar Still A Comparative Study. Int J Engg Techsci, 2011, 2(2), 161-168

[13] S Kumar, GN Tiwarim Estimation of convective mass transfer in solar distillation system, Solar Energy, 1996, 57, 459-464.

[14] AK Tiwari, GN Tiwari, Effect of water depths on heat and mass transfer in a passive solar still in summer climatic condition. Desalination 195, 2006, 78-94

[15] N Setoodeh, R Rahimi, A Ameri, Modeling and determination of heat transfer coefficient in a basin solar still is using CFD. Desalination 268, 103-110, 2011

[16] Jadav Madhav, Performance of Black Granite Basin Solar Still International Journal of Tech Science, 2(2), 161-168, 2011

[17] Omar Badran, Theoretical Analysis of Solar Distillation Using Active Solar Still, International Journal of Thermal & Environment Engineering, 2011, 3(2), 113-120